Talanta 125 (2014) 265–275

Contents lists available at ScienceDirect

Talanta

journal homepage: www.elsevier.com/locate/talanta

Comprehensive plasma profiling for the characterization of graft-versus-host disease biomarkers

Muriel De Bock [a], Yves Beguin [a,b], Pierre Leprince [a], Evelyne Willems [b], Frédéric Baron [a,b], Céline Deroyer [a], Laurence Seidel [c], Etienne Cavalier [d], Dominique de Seny [a], Michel Malaise [a], André Gothot [a], Marie-Paule Merville [a], Marianne Fillet [a,e,*]

[a] GIGA Research (GIGA-I³, GIGA-cancer, and GIGA-Neuroscience), University of Liège, CHU, B36, B-4000 Liège, Belgium
[b] Department of Medicine, Division of Hematology, University and CHU of Liège, Liège, Belgium
[c] Department of Statistics, University of Liège, CHU, B-4000 Liège, Belgium
[d] Department of Clinical Chemistry, CHU of Liège, CHU, B-4000 Liège, Belgium
[e] Department of Analytical Pharmaceutical Chemistry, CIRM, Institute of Pharmacy, University of Liège, CHU, B36, B-4000 Liège, Belgium

ARTICLE INFO

Article history:
Received 13 October 2013
Received in revised form
28 February 2014
Accepted 11 March 2014
Available online 18 March 2014

Keywords:
Graft-versus-host disease
Biomarkers
Composite panel
Clinical proteomics

ABSTRACT

Acute graft-versus-host disease (aGVHD) remains a life-threatening complication of hematopoietic stem cell transplantation (HSCT) therefore limiting its application. To optimize the management of aGVHD and reduce therapy-related toxicity, early specific markers are needed. The main objective of this study was to uncover diagnostic biomarkers by comparing plasma protein profiles of patients at the time of acute GVHD diagnosis with those of patients undergoing HSCT without aGVHD. Additional analysis of samples taken 15 days before aGVHD diagnosis was also performed to evaluate the potential of our newly discovered biomarkers for early diagnosis. To get complementary information from plasma samples, we used three different proteomic approaches, namely 2D-DIGE, SELDI-TOF-MS and 2D-LC-MS^E.

We identified and confirmed by the means of independent techniques, the differential expression of several proteins indicating significantly increased inflammation response and disturbance in the coagulation cascade. The variation of these proteins was already observed 15 days before GVHD diagnosis, suggesting the potential early detection of the disease before symptoms appearance.

Finally, logistic regression analysis determined a composite biomarker panel comprising fibrinogen, fragment of fibrinogen beta chain, SAA, prothrombin fragments, apolipoprotein A1 and hepcidin that optimally discriminated patients with and without GVHD. The area under the receiver operating characteristic curve distinguishing these 2 groups was 0.95.

1. Introduction

Allogeneic hematopoietic stem cell transplantation (HSCT) has been included in the therapeutic arsenal of hematological malignancies and genetic disorders for many years. Although this therapeutic approach has demonstrated good rates of success for disease eradication, life-threatening complications such as severe infections or graft-versus-host disease (GVHD) remain a major problem after HSCT.

GVHD can be defined as an exacerbated immune reaction mediated by the infused donor immunocompetent cells present in a genetically different and immunosuppressed host. Damaged host cells and bacterial products such as bacterial lipopolysaccharides induce the secretion of proinflammatory chemokines and cytokines, such as TNF-alpha, IL-1 and IL-6 that activate antigen-presenting cells. Presentation of host alloantigens to donor T cells leads to their proliferation and differentiation, thereby inducing a “cytokine storm” leading finally to the activation of cellular effectors amplifying host tissue injury [1–3]. Skin, liver and gastrointestinal tract are the main organs affected by acute GVHD. The staging of this pathology is based on the localization and the severity of injury.

Although improvements have been achieved in the prevention of GVHD through the use of new immunosuppressive drugs or changes in the source of cells and graft manipulation [4–6], prophylactic approaches appear to be insufficient to avoid any

Abbreviations: aGVHD, acute graft-versus-host disease; Apo, apolipoprotein; APP, acute phase protein; ASB-14, amidosulfobetaine-14; CRP, C-reactive protein; F13B, coagulation factor XIII beta chain; FBG, fibrinogen; FGB, fibrinogen beta chain; HAMP, hepcidin antimicrobial peptide; HRG, histidine-rich glycoprotein; HSCT, hematopoietic stem cell transplantation; LC-MS, liquid chromatography–mass spectrometry; PLG, plasminogen; SAA, serum amyloid A; SELDI-TOF-MS, surface enhanced laser desorption ionisation-time of flight-mass spectrometry

* Corresponding author at: Laboratory of Analytical Pharmaceutical Chemistry, Department of Pharmacy, University of Liège, CHU, B36, B-4000 Liège, Belgium. Tel.: +3243664345.
E-mail address: Marianne.fillet@ulg.ac.be (M. Fillet).

http://dx.doi.org/10.1016/j.talanta.2014.03.017
0039-9140/

complications. Moreover, such improvements are accompanied by an increased rate of relapse due to the close correlation between GVHD and graft-versus-tumor effects [7,8], thereby compromising HSCT efficacy. Although consensus has emerged supporting the use of high-dose (methyl)prednisolone or prednisone for initial treatment of acute GVHD, practices differ among centers with respect to the initial glucocorticoid dose to be applied, the use of additional immunosuppressive agents, the management of treatment withdrawal after initial improvement, and the treatment of patients who failed to respond to steroids [9]. Second line of treatment for steroid-refractory aGVHD includes increased dose of immunosuppressive agent (cyclosporine, mycophenolate mofetil or tacrolimus), antithymocyte globulin, monoclonal antibodies as well as extracorporeal photophoresis or mesenchymal stem cell infusion [10]. For all these reasons, GVHD remains a challenge for clinicians in the application of HSCT.

Currently, diagnosis and grading of acute GVHD are based on clinical manifestations and histopathological analysis of involved organ biopsies [11]. Those are time-consuming, invasive and poorly specific practices. Measurement of biomarkers from fluids such as blood or urine could be a useful tool to diagnose and even predict the GVHD onset allowing an earlier initiation of treatment and a better management of this complication. Moreover, the identification of new biomarkers of GVHD could give novel insights on the underlying mechanisms and physiological processes of this pathology.

Although many studies report the monitoring of chemokines and cytokines as potential acute GVHD (aGVHD) biomarkers [12–17], only few investigations based on non-targeted proteomic approaches have been performed [18–25]. Among those, Weissinger et al. identified in urine modulation of peptide expression generated from collagen, albumin, beta2-microglobulin and CD99, indicating significant disturbances in collagen metabolism and T-cell activation [18,22,26]. Moreover, recent studies from Ferrara's group by cytokine antibody microarrays and Intact Protein Analysis System identified a panel of GVHD plasma biomarkers (namely IL-2 alpha, TNFR1, HGF, IL-8, elafin and reg3alpha) [15,19,23]. Those markers were validated and could discriminate therapy responsive from non-responsive patients and predict survival in patients receiving GVHD therapy [27,28].

Non-targeted proteomic approaches present the advantage to examine in a single experiment a large panel of peptides and proteins, providing a fingerprint of a pathophysiological situation at a given time. As a single biomarker could be the indicator of many unrelated pathological changes, the simultaneous detection of several markers is a key to improve specificity [29]. In this particular disease and considering the diversity of complications after HSCT, combination of biomarkers should assure a more specific diagnosis.

In this study, a non-targeted proteomic approach was used with the objective to find diagnostic markers of GVHD and to highlight physiopathological mechanisms of the disease. As there are numerous factors of variability associated to HSCT, very well characterized (GradeII aGVHD) and homogeneous groups (conditioning regimen intensity, donor, preventive treatment therapy,…) were build. Plasma protein profiles from patients with aGVHD were compared with those of patients undergoing HSCT without any aGVHD symptoms. Additional analysis of samples taken 15 days before aGVHD diagnosis was also performed to evaluate the potential of our newly discovered biomarkers for early diagnosis. To extract a maximum of information from plasma samples, three complementary proteomic approaches: a gel-based (2D-DIGE) and two MS-based (SELDI-TOF-MS and 2D-LC-MS^E) approaches were undertaken.

2. Materials and methods

2.1. Patients and sample collection

2.1.1. Ethics

Written informed consent was obtained from each patient to undergo allo-HSCT and to collect, store and analyze blood samples

Table 1
Patient characteristics: control vs Grade II aGVHD.

Characteristics	2D-DIGE		SELDI-TOF-MS		2D-LC-MS^E		Western blot	
	***Control* (*n*=16)**	***aGVHD* (*n*=16)**	***Control* (*n*=16)**	***aGVHD* (*n*=16)**	***Control* (*n*=23)**	***aGVHD* (*n*=23)**	***Control* (*n*=28)**	***aGVHD* (*n*=28)**
Median age, years (range)	58 (16–66)	57 (21–67)	63 (30–66)	61 (23–70)	61 (30–72)	61 (23–70)	60 (30–72)	60 (21–70)
Gender								
Male	13	14	11	14	15	16	20	20
Female	3	2	5	2	8	7	8	8
Diagnosis								
Acute myeloblastic leukemia	6	4	7	4	9	5	13	7
Lymphoma	2	5	3	6	3	7	4	9
Multiple myeloma	4	5	1	2	4	4	5	5
Myelodysplastic syndrome	0	0	1	3	2	5	1	4
Other malignancies	4	2	4	1	5	2	5	3
Donor								
Related	4	7	3	3	4	5	6	8
Unrelated	12	9	13	13	19	18	22	20
Conditioning regimen intensity								
Myeloablative	4	5	0	0	0	0	4	5
Reduced	12	11	16	16	23	23	24	23
ATG administration	6	6	0	0	0	0	6	5
Acute GVHD								
Skin		15		12		19		22
Gut		7		7		7		9
Liver		1		0		0		2
Combined		7		3		3		5
Day of onset of acute GVHD, median (range)		34 (13–139)		46 (15–245)		47 (15–245)		44 (13–245)
Post-HSCT day of samples, median (range)	34 (10–139)	36 (14–139)	46 (21–259)	46 (18–248)	47 (21–259)	47 (18–248)	45 (10–259)	44.5 (14–248)

for research purposes. The Ethics Committee of the University of Liège ("Comite d'Ethique Hospitalo-Facultaire Universitaire de Liège") approved the consent form as well as the current research study protocol (protocol #B707201112193).

All patients were transplanted at the University Hospital Center of the University of Liège with peripheral blood stem cells following myeloablative or reduced-intensity conditioning regimens for haematological malignancies. Patients with active infection on sampling day were excluded. Diagnosis and grading of acute GVHD were based on clinical symptoms and biopsies according to established criteria [11].

EDTA plasma samples were prospectively collected weekly until day 100 after HSCT and every 2 weeks until day 365 from April 2007 to September 2011. aGVHD samples were taken on the day of diagnosis, before corticosteroid administration (GVHD D0). Patients considered as controls (patient under HSCT without aGVHD) were matched for sex, age, conditioning intensity regimen and time of sample collection after HSCT. Patient characteristics are summarized in Table 1. As samples were collected until September 2011, studied cohorts were adapted gradually for the different analyses including new samples and homogenising groups of patients.

2.2. 2D-DIGE proteomic approach

2.2.1. Set of patients and plasma processing

Thirty-two patients including 16 with grade II aGVHD at D0 and D-15 and 16 control patients were enrolled.

In order to deplete very abundant plasma proteins, which could disturb the electrophoretic process, a bead-based combinatorial peptide library technology (ProteoMiner®, Biorad Laboratories Inc., Hercules, CA, USA) was applied according the manufacturer's recommendations [30]. After removal of the unbound fraction with PBS buffer (3×5 min of incubation), proteins were eluted with 3×100 μL of a 2D DIGE compatible elution solution (25 mM Tris, 7 M urea, 2 M thiourea, 4% CHAPS) to avoid a subsequent desalting step.

2.2.2. D-difference gel electrophoresis (2D-DIGE) analysis

Four pools of each sample groups (control, grade II GVHD D0 and D-15) were separated by 2D-DIGE. Protein content was determined using PlusONE 2-D Quant Kit (GE Healthcare, Uppsala, Sweden). Twenty-five μg of proteins from each pool were labelled separately with 0.2 nmol of Cy3 or Cy5 dyes for an incubation time of 30 min. The reaction was stopped by adding 10 mM lysine. To avoid experimental variation, an equal distribution of Cy3 and Cy5 dyes between control and GVHD samples was realized. An internal standard labelled with Cy2 dye was prepared with equal amounts of proteins from each sample included in the experimental procedure. After combining the internal standard with labelled control and GVHD samples, the volume was adjusted to 450 μl by adding rehydration buffer (7 M urea, 2 M thiourea, 2% (w/v) ASB 14, 1.2% (v/v) Destreak reagent and 0.6% (v/v) pH 3-10 NL IPG buffer). This was added to a 24 cm pH 3-10 NL strip for passive rehydration for 8 h at 20 °C. Isoelectric focusing (IEF) was conducted at 500 V for 1 h, gradient 1 kV for 3 h, gradient 8 kV for 3 h and constant 8 kV for 8 h 45 at 20 °C with a maximum current setting of 50 μA per strip (IPGphor isoelectric focusing unit, GE Healthcare). After the first dimension separation, IPG strips were equilibrated in a solution made up of 6 M urea, 50 mM Tris pH 8.8, 30% glycerol, 1.6% sodium dodecyl sulfate and a trace of bromophenol blue, containing first 1% dithiothreitol (DTT) and then 5% iodoacetamide, each time for 15 min. Second dimension electrophoresis was performed by overnight orthogonal SDS-PAGE of the proteins on 12% (w/v) acrylamide gels at 20 °C in an Ettan Dalt II system (GE Healthcare) at 1 W/gel.

2.2.3. Gel and data analysis

Spot profile images were obtained with a Typhoon 9400 Laser Scanner (GE Healthcare) by scanning at three different wavelengths corresponding to the emission spectrum of the three CyDyes. Image and data analysis were performed using DeCyder software (GE Healthcare). After spot detection, normalisation of spot volumes with the internal standard and log transformation of protein abundance, each normalised spot volume was compared between groups and a p-value and a spot intensity ratio (GVHD/control spot intensities) were assigned. Spots with a 1.5-fold increase or decrease in normalized spot volume and a significant statistical difference (p-value < 0.05) calculated by Student t-test analysis were considered as spot of interest. This is the commonly used approach for 2D-DIGE data analysis [31]. Statistical significance of GVHD D0 versus GVHD D-15 comparison was evaluated using paired t-test.

2.2.4. Protein identification

Preparative gels containing unlabelled proteins and the internal standard were run in parallel and used for excision of spots of interest with the Ettan Spot Picker robot (GE Healthcare). Trypsin in-gel digestion was performed on the Janus working station (Perkin Elmer, Waltham, MA, USA). Pieces of gel were successively washed with 50 mM NH_4HCO_3 following by 50 mM NH_4HCO_3/ACN (50/50) solution. After reduction with 50 mM DTT and alkylation with 55 mM iodoacetamide, gels were washed as previously described and dried out with ACN. Then digestion with trypsin (Promega, Madison, WI) was performed and peptides dissolved in a 0.1% TFA solution were recovered and spotted on a MALDI plate prior to the addition of 1 μL of R-cyano-4-hydroxycinnamic acid (CHCA) (7 mg/mL, 50% v/v ACN, 0.1% v/v TFA, Sigma Aldrich, MO).

PMF and MS/MS analysis were performed on an MALDI-TOF-TOF-MS, Ultraflex II (Bruker Daltonics, Billera, MA, USA) operated in positive ion mode. Automatic spectra acquisition was piloted with the Flex control ™ v3.0 software and real time analysis by Flex analysis ™ v3.0 software (Bruker Daltonics). Searches on databases were managed in real time with BioTools ™ v3.1 (Bruker Daltonics) on the Mascot server v2.2.2. Identification searches were performed on the Swissprot database restricted to Human taxonomy with 100 ppm of mass accuracy in MS and 300 ppm in MS/MS. The 4 most intense peaks detected within each PMF were selected for MS/MS [32,33].

2.3. SELDI-TOF-MS proteomic approach

2.3.1. Set of patients and plasma processing

Thirty-two patients undergoing HSCT after reduced intensity conditioning were included. Plasma samples were divided in three groups: controls ($n=16$), GVHD D-15 ($n=11$) and GVHD D0 ($n=16$) (Table 1). Plasma samples were processed individually with Proteominer® and proteins were eluted with a solution made of 8 M urea, 2% CHAPS and 5% acetic acid.

2.3.2. SELDI-TOF-MS analysis

Each sample was analysed individually. Protein profiles were generated using CM10 cation ion exchange array (Biorad Laboratories Inc.) with complementary pH 4 and pH 9 binding conditions as described in a previous study [34]. Briefly, samples were diluted ten times in either 100 mM sodium acetate binding buffer (pH 4) or in Tris–HCl 100 mM binding buffer (pH 9) and analysed in duplicate. To control technical variations, a plasma sample treated by ProteoMiner® was run on multiple arrays and was used as

quality control. Diluted samples were incubated for 1 h on chromatographic surfaces activated with the corresponding binding buffer. Spots were washed with appropriate binding buffers and milli-Q water and air dried. Finally, saturated sinapinic acid matrix solution was applied. Two ranges of mass low-mass (LM: 2000–8000 Da) and medium mass (MM: 8000–30,000 Da ranges) were processed separately according to the two calibration equations generated externally using All in one peptide and All in one protein standard (Biorad Laboratories Inc.). Spectra were acquired using PCS4000 SELDI-TOF-MS (Biorad Laboratories Inc.) by averaging 1200 shots at laser intensity of 4400 (LM) and 5000 (MM) for pH 4 condition and 4200 (LM) and 5000 (MM) for pH 9 condition. Focus mass was set for low and medium mass range at 4500 Da and 10,000 Da, respectively. Data were processed using Proteinchip Data Manager Software (Biorad Laboratories Inc.). After baseline subtraction, noise calculation, spectra alignment and total ion current normalisation, peak clusters were formed by optimizing peak detection for each condition. *p*-Values were calculated using the non-parametric Mann–Whitney test based on the cluster median intensity of each spectra group. Protein data manager software uses nonparametric tests and takes into account only the ranking of the intensities during the *p*-value calculation. This statistical test does not assume a normal distribution of ProteinChip SELDI data.

2.3.3. Protein identification by immunodepletion

The proteomic study detected four proteins at different *m*/*z* ratios as putative biomarkers and a range of biochemical methods were used to characterize and identify these markers as described in Supplementary data S1.

2.4. 2D-LC-MS^E proteomic approach

2.4.1. Set of patients, plasma processing and data collection

A total of 46 patients, 23 control patients and 23 patients with grade II aGVHD were included in this analysis. All samples analysed by SELDI-TOF-MS were enrolled in this cohort. Crude plasma samples were equally divided (7-8-8) to constitute three pools for each group (control and GVHD D0) (Table 1). After protein quantification using RCDC kit (Biorad), 1500 μg of total protein per sample were depleted of high abundant proteins using Seppro IgY14 spin column kit (Sigma-Aldrich, St. Louis, MO, USA) applying manufacturer protocol two times. After reduction, alkylation and complete protein trypsin digestion, peptide digests were desalted on C18 Zip Tip (Millipore, Billerica, CA, USA). The eluted peptides were finally diluted in 100 mM ammonium formiate adjusted at pH 10 with ammonia and spiked with a commercial mix of 4 protein digests. To monitor sample processing, 15 μg of *Bacillus licheniformis* α-amylase and 21 μg of *Saccharomyces cerevisiae* invertase were added to samples prior depletion and digestion steps respectively.

Analysis were performed using a nanoAcquity system (Waters Corporation, Mildford, MA, USA) coupled with the Q-TOF Synapt HDMS™ G1 system mass spectrometer (Waters Corporation). Configuration of the 2D-nano UPLC system was a reverse phase pH 10/reverse phase pH 3 based 2D separation. First, samples were loaded at 2 μL/min (20 mM ammonium formiate, pH 10) on a X-Bridge BEH C18 5 μm column (300 μm, 50 mm) followed by five acetonitrile gradient elution steps (10, 14, 16, 20 and 65%). Each fraction was desalted and equilibrated at pH 3 online on a trapping column Symmetry C18 5 μm (180 μm, 20 mm) before separation on the second analytical column (BEH C18 1.7 μm (75 μm, 250 mm): flow rate 300 nL/min, solvent A (0.1% formic acid in water) and solvent B (0.1% formic acid in acetonitrile), gradient 0 min, 97% A; 90 min, 60% A.

Data were acquired by collecting spectra every 1 s in a data-independent MS^E positive mode with alternating low and elevated energy (ramping) over a 50–1500 *m*/*z* range. The UniProtKB database search for protein identification involves trypsin as protease, with 1 possible misscleavage, with carbamydomethylation (C) as fixed modification and oxidation (M) and phosphor (STY) as variable ones. Raw data were processed (deconvoluted, deisotoped) and the protein identification and relative quantification were performed using ProteinLynx Global SERVER (PLGS) v2.5. The following parameters were used: PLGS differential quantitative relative analysis was performed with the assumption that a protein is identified and quantified and reached significance in the comparison using the three biological replicates per sample group. The relative abundance was calculated for each identified protein and expressed as ratio based on the mean ± SD of the expression of each protein from the replicate values. The calculated *p*-values determined the probability of regulation, a *p*-value associated to the difference of ratio or LogE ratio < 0.05 or > 0.95 indicated a 95% likelihood of downregulation or a 95% likelihood upregulation, respectively.

2.5. Protein determination

2.5.1. Western blotting (WB)

Potential biomarkers revealed by 2D-DIGE, SELDI-TOF-MS and 2D-LC-MS^E were tested by WB on 56 individual crude plasma samples (28 controls, 28 aGVHD). This set of samples included 32 plasma from the 2D-DIGE analysis and 24 non-redundant samples tested by SELDI-TOF-MS and 2D-LC-MS^E. Equal volumes of plasma samples from control and aGVHD patients were loaded on sodium dodecyl sulfate (SDS)-polyacrylamide gel. Proteins were transferred on polyvinylidene difluoride membranes (Millipore) and then blocked in 5% milk solution for 1 h. Membranes were incubated with primary antibodies: mouse monoclonal anti-plasminogen (1/1000), mouse monoclonal anti-coagulation Factor XIII (1/200), goat polyclonal anti-fibrinogen beta chain (1/200) (Santa Cruz biotechnology, Santa Cruz, CA, USA), rabbit monoclonal anti-serum amyloid A4 (1/1000) and histidine-rich glycoprotein (1/1000) (Abcam). After washing the membranes, corresponding horseradish peroxidase-conjugated secondary antibodies were added with a dilution of 1/10,000 for mouse and rabbit (GE Healthcare) and 1/2000 for goat (Dako, Glostrup, Denmark) antibodies. Western blot band signals were revealed using enhanced chemiluminescence detection reagent (ECL kit, Thermo Scientific, MA) and were detected by Imaquant LAS 4000 Mini luminescence image analyzer (GE Healthcare). The intensity of each band was measured using Imagequant TL® software (GE Healthcare). Statistical analysis was performed by the Mann–Whitney test using Prism 4.00 Software (Graph pad, San Diego, CA, USA), with statistical significance accepted at $p < 0.05$.

2.5.2. Measurement of hepcidin-25 in plasma samples by LC-MS/MS

Hepcidin-25 levels of 54 plasma samples (28 controls and 26 aGVHD samples) were measured by a LC-chip coupled to a nanoelectrospray/ion trap/MS operating in positive mode. Extraction procedure, calibration standard preparation, chromatographic and MS parameters were previously described by Houbart et al. [35].

2.5.3. Quantification of SAA and apolipoprotein A1 levels by ELISA

SAA1 and Apo A1 levels were measured by ELISA in serum samples from 28 controls and 28 aGVHD at the time of aGVHD onset. In addition, these proteins levels were also evaluated in 19 serum samples taken 15 days before aGVHD onset. SAA1 and Apo A1 levels were measured by ELISAs following the manufacturer's protocol (Life Technologies, Carlsbad, CA, USA/Abnova, Taipei city, Taiwan). Samples were diluted 1:200 and 1:100 for SAA

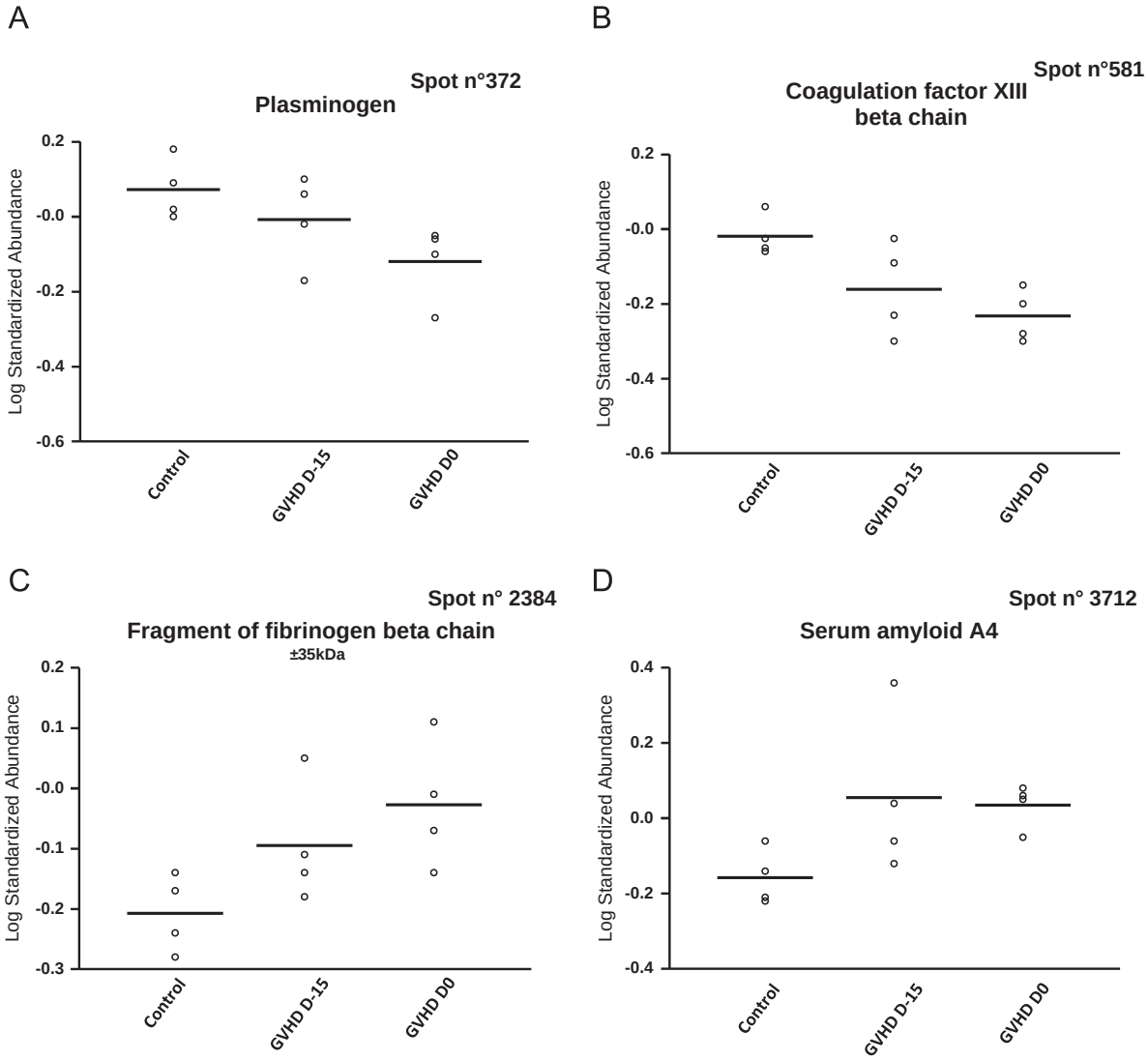

Fig. 1. Relative abundance of 2D-DIGE differentially expressed protein spots for control and GVHD patient samples. Protein abundance of each spot was first standardized against the internal standard before log transformation. After statistical analysis using Student *t*-test analysis, significantly differentially expressed proteins (p-value < 0.05) were identified by MALDI-TOF-TOF as plasminogen (A), coagulation factor XII beta chain (B), fibrinogen beta chain (C) and serum amyloid A4 (D). Each graph shows the log standardized protein abundance of each biological replicates (o) and the mean value (—). GVHD D0 and GVHD D-15 are respectively the day of the aGVHD diagnosis and 15 days before.

and Apo A1 assays, respectively. Patient samples whose cytokine levels were out of standard curve range, were re-assessed after dilution.

2.5.4. *Quantification of fibrinogen, CRP and prothrombin fragments 1+2 in plasma samples*

Levels of C-reactive protein (CRP), fibrinogen and prothrombin fragments 1+2 were assessed in samples from 28 controls and 28 aGVHD patients. Samples from aGVHD group were taken at time of GVHD diagnosis and 15 days before. Heparinized and citrated plasma samples were used for CRP and fibrinogen measurement respectively. CRP level was evaluated by immunoturbidimetric assay using modular Roche P (Roche Diagnostics, Indianapolis, IN, USA). Reference range is 0–6 mg/L. Citrated plasma fibrinogen level was measured by Clauss method using BCS system (Siemens, Deerfield, IL). Normal level ranges between 2.3 and 4.3 g/L. Additionally, quantification of prothrombin fragments was performed on EDTA plasma by ELISA assay (Enzygnost F1+2 monoclonal, Siemens).

2.5.5. *Pathway analysis*

Data sets of differentially expressed proteins and their respective ratio change were examined by the "Core analysis" function of Ingenuity Pathway Analysis software (Ingenuity Systems, Redwood city CA, USA) in order to place proteins into molecular networks, similar signaling and metabolic pathways as well as biological function classes.

2.6. *Statistical analyses*

Univariate and multivariate statistical analyses were used to evaluate the ability of the markers to predict the onset of aGVHD based on sample values obtained by Western Blot, ELISA, LC-MS/MS and routine tests ($n=56$). Proteins included in the analysis were plasminogen, coagulation factor XIII, fibrinogen beta chain fragment (± 35 kDa), SAA4, SAA1, CRP, fibrinogen, histidine-rich glycoprotein, prothrombin F1+2, hepcidin and apolipoprotein AI. Biomarkers with skewed distributions were log-transformed and then used as continuous covariates in logistic regression models. Multivariate logistic regression model with stepwise selection was

applied to generate the best composite panel of biomarkers that discriminated between control and aGVHD samples. Area under the curve (AUC) for individual markers as well as for the composite panel was computed using logistic regression. Correlation coefficients and associated *p*-value were determined by non parametric Spearman's correlation test.

3. Results

3.1. Biomarker detection

3.1.1. 2D-DIGE analysis

2D-DIGE was used to provide plasma protein distribution patterns ranging from 15 kDa to 150 kDa. In the comparison between four pools of grade II aGVHD D0 and control patients (four patients per pool), four differentially expressed proteins were identified: plasminogen, coagulation factor XIII beta chain, fibrinogen beta chain fragment and serum amyloid A4 (Fig. 1A–D and Table 2). While the first two proteins were found to be less abundant in grade II GVHD plasma samples, the two others were more abundant. The four identified proteins in GVHD D-15 samples were at an intermediate protein level between controls and aGVHD D0 (Fig. 1A–D).

3.1.2. SELDI-TOF-MS analysis

Plasma samples from 16 control patients and 16 patients with grade II aGVHD were individually analysed by SELDI-TOF-MS. Peak intensities of 36 *m*/*z* values were found to discriminate significantly the control and aGVHD D0 samples. Peaks at *m*/*z* of 2792, 11687, 17271 and 28120 were identified to be hepcidin-25, serum amyloid A1, a truncated form of apolipoprotein AII homodimer and apolipoprotein AI, respectively (Table 2, Supplementary data S1). Identification of hepcidin-25 was additionally confirmed by LC-MS/MS. As depicted in Fig. 2A and B, the peak intensities of hepcidin and SAA1 were found to be significantly increased on the day of aGVHD diagnosis. In addition, their peak intensities were already found higher in GVHD D-15 samples compared to controls. Peak intensities of apolipoprotein AI and AII were found to be decreased in GVHD D0 and also in GVHD D-15 samples suggesting an early change in protein levels.

3.1.3. 2D-LC-MS^E analysis

Six pools of samples, 3 grade II aGVHD D0 and 3 controls were compared using a label-free quantitative LC-MS^E approach (seven or eight patients per poll). Ninety proteins were found differentially expressed and were identified (Supplementary data S2). Fifty six proteins were downregulated whereas 34 were upregulated in the aGVHD group. Six significant canonical pathways were identified to be involved in aGVHD are acute phase response signalling, LXR/RXR activation, coagulation system, intrinsic and extrinsic prothrombin pathway activation as well as primary immunodeficiency signalling. Levels of some negative acute phase proteins (APP), such as histidine rich glycoprotein (HRG), transthyretin and retinol-binding protein 4, were found to be lower in GVHD D0 samples, while levels of positive APP such as α1-antitrypsin, haptoglobin or complement components were found increased. CRP was the most increased protein in aGVHD samples (ratio: 3.39). In addition, some proteins involved in coagulation were altered in aGVHD (see Supplementary data S2). Interestingly, plasminogen level was found to be decreased while levels of various fibrinogen chains increased in GVHD D0 samples, which is in accordance with 2D-DIGE results.

Finally, 11 potential biomarkers identified by the three proteomic approaches were selected (Table 2).

3.2. Biomarker confirmation

Five proteins of interest, detected as potential biomarkers by the previous proteomic approaches, were quantified in 56 crude plasma samples (28 controls and 28 grade II aGVHD) by Western blot. Fig. 3A–D shows quantification results for plasminogen, coagulation factor XIII, hepcidin and SAA1, which confirmed the significant differential plasma levels observed in the two groups. Moreover, an increase of SAA4 and fibrinogen beta chain fragment levels as well as decreased levels of HRG and Apo AI were also observed but were not statistically significant (data not shown).

C-reactive protein (CRP) and fibrinogen levels detected by LC-MS^E and 2D DIGE were confirmed by clinical routine assays. As expected, these two markers of inflammation increased at the onset of aGVHD compared to controls (CRP and fibrinogen *p*-values were 0.0017 and NS, respectively) (Fig. 3E). Interestingly, it can be noticed that CRP and SAA1 showed a slight (not significant) increase 15 days before aGVHD onset (data not shown). Moreover, to assess a potential activation of coagulation at the time of aGVHD occurrence, prothrombin fragments 1+2 levels were measured in controls, GVHD D-15 and GVHD D0 samples. A non-significant increase of these activation peptide fragments was observed at aGVHD onset.

3.3. Correlation

Pairwise associations between different biomarkers in samples taken on the day of aGVHD diagnosis were evaluated using the Spearman's test and are listed in Table 3.

Significant positive correlations were found between CRP, an acute phase reactant, and other inflammation-related proteins such as SAA1, hepcidin and fibrinogen. On the opposite, CRP level correlated negatively with coagulation-related factors such as plasminogen and factor XIII. Although SAA1 correlated with CRP, prothrombin F1+2, another member of the SAA family, SAA4, showed no correlation with inflammatory markers but only with coagulation factor XIII. As expected, plasminogen positively correlated with coagulation factor XIII and histidine-rich glycoprotein, both are involved in coagulation. Apolipoprotein AI levels, implied in cholesterol transport, were associated with both hepcidin and HRG.

3.4. Logistic regression analysis and ROC curves with multiple markers

Multivariate logistic analysis realized on the 11 identified biomarkers determined that a combination of SAA1, prothrombin F1+2, fibrinogen beta chain fragment, Apo A1, fibrinogen and hepcidin levels produced the best model to predict the occurrence of aGVHD. SAA1 was found to have the best predictive value (AUC=0.74) as single biomarker. Interestingly, the generated composite panel markedly increased the AUC to 0.95 (Fig. 4).

4. Discussion

Although HSCT is a therapy of choice for various malignant or genetic haematological disorders, its application requires a lot of expertise to limit life-threatening complications such as acute graft-versus-host disease. This is why an early and specific diagnosis of aGVHD could help clinicians to optimize management of that disorder and reduce therapy-related toxicity.

As summarized in Table 2, the combination of three proteomic analysis approaches provided a panel of differentially expressed proteins between patients developing aGVHD or not after HSCT. Interestingly, each proteomic approach provided complementary

information while some differentially expressed proteins such as plasminogen or fibrinogen chains were consistently found between analyses, demonstrating their reliability.

Decrease of plasminogen and coagulation factor XIII levels as well as increase of fibrinogen beta chain and serum amyloid A4 levels (Fig. 1) were observed by 2D DIGE. Then, SELDI-TOF-analysis revealed variation of hepcidin, SAA1, apolipoprotein I and II at aGVHD onset. In addition, analysis performed using LC-MS^E detected 90 proteins that are differentially expressed between controls and aGVHD patients among others plasminogen, histidine-rich glycoprotein, fibrinogen chains and CRP. Finally, the differential expression of our proposed biomarkers detected by proteomic approaches were further confirmed on a larger cohort of samples ($n=56$) using targeted methods (ELISA, Western blot or LC-MS/MS). It has to be noticed that we only focused on some differentially expressed proteins revealed by LC-MS^E experiment, mainly confirming observations made by 2D-DIGE and SELDI-TOF-MS. However, further investigations should be performed for the other potential biomarkers such as gelsolin or lumican (cf. Supplementary data S1). Indeed, these proteins could reflect endothelial impairment as they are related to inflammation, apoptosis [36] or collagen fibrillogenesis [37] making these biomarkers interesting.

As presented in Fig. 5, newly discovered aGVHD biomarkers are mainly involved in two interrelated biological processes: inflammation and coagulation processes [38]. Moreover, changes in abundance of apolipoprotein A1 and SAA4 levels also suggest an alteration of lipid metabolism following aGVHD onset [39,40].

Levels of positive acute phase reactants of inflammation (SAA1, CRP and HAMP) were found elevated with the occurrence of aGVHD while some coagulation factor levels decreased (PLG and F13B). The alteration of these protein levels are in agreement with previous reviews describing the complex pathophysiology of GVHD [1,3,41,42]. Indeed, the complex mechanism of GVHD

Table 2
Summary of the biomarkers identified for Grade II GVHD.

Proteomic approach	Biomarkers identity	Abbreviations	*p*-Value	Up (>1)—or down (<1) regulated in GVHD
2D-DIGE	Coagulation factor XIII B chain	F13B	0.044[a]	0.58
	Fibrinogen beta chain	FGB	0.026[a]	1.54
	Plasminogen	PLG	0.025[a]	0.65
	Serum amyloid A4	SAA4	0.006[a]	1.54
SELDI-TOF-MS	Apolipoprotein A1	APOA1	0.007[b]	0.81
	Hepcidin	HAMP	0.021[b]	1.75
	Serum amyloid 1	SAA1	0.002[b]	5.30
2D-LC-MS^E	C-reactive protein	CRP	>0.95[c]	3.39
	Fibrinogen beta chain	FGB	>0.95[c]	1.31
	Histidine rich glycoprotein	HRG	<0.05[c]	0.76
	Plasminogen	PLG	<0.05[c]	0.90

[a] Student *t*-test.
[b] Mann–Whitney test and
[c] Markov Chain Monte Carlo exploration (*p*-value <0.05 (downregulated) or >0.95 (upregulated) were considered as being significant.

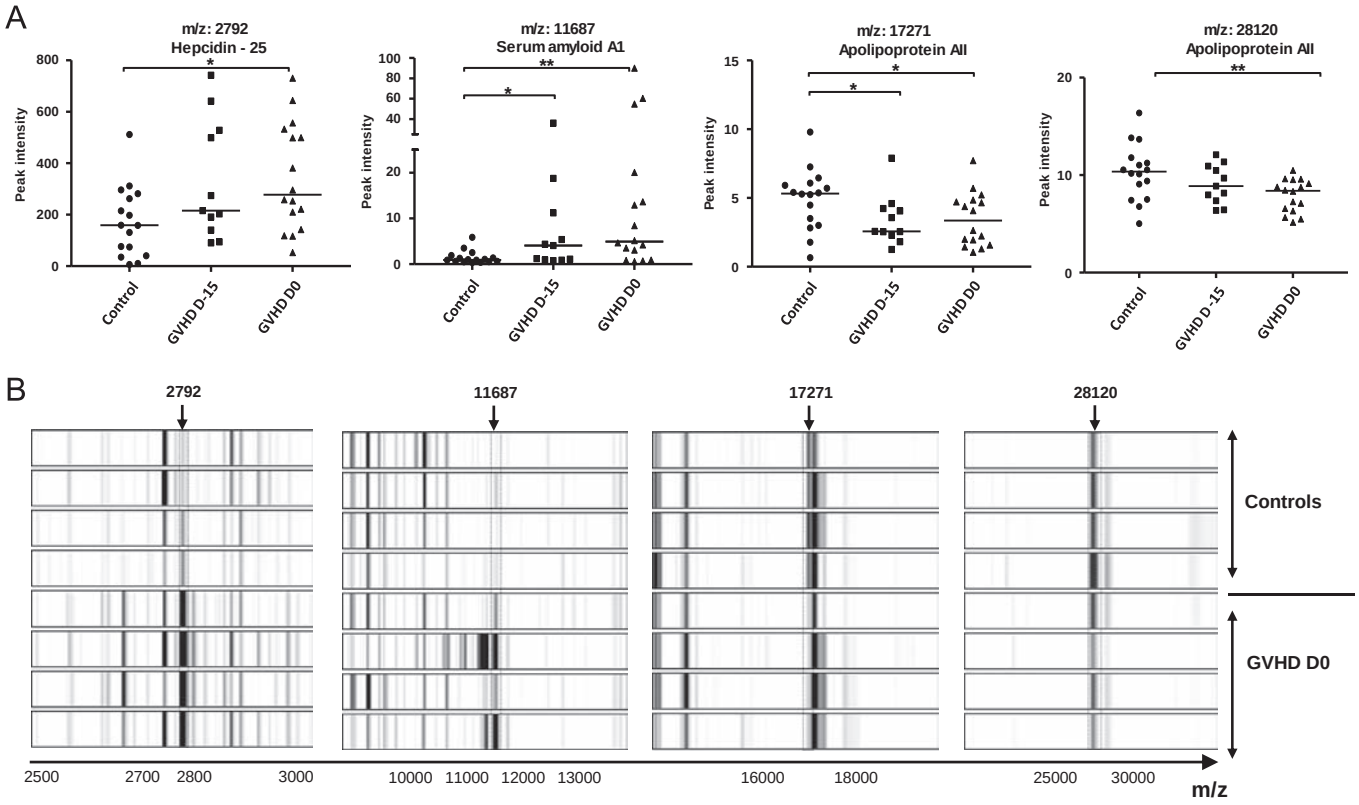

Fig. 2. Differential protein abundance observed by SELDI-TOF-MS between control and GVHD patient samples. Spectra from controls, 15 days before GVHD diagnosis (D-15) and the day of GVHD diagnosis (D0) samples were obtained by SELDI-TOF-MS analysis using CM10 ProteinChip Array in two pH conditions of binding: pH4 and pH9. Statistical significance (*p*-value <0.05) was calculated by a Mann–Whitney test. * $p<0.05$; ** $p<0.01$; *** $p<0.001$. (A) Graphs depict, for each biological replicates (●), the intensities of four statistically significant SELDI-TOF-MS peaks, subsequently identified as hepcidin-25 (*m*/*z* 2792), serum amyloid A1 (*m*/*z* 11687), apolipoprotein AII (*m*/*z* 17271) and apolipoprotein AI (*m*/*z* 28120). Median value (—) of peak intensities are depicted for controls, D-15 and D0 aGVHD samples. (B) Representative gel view spectra representing peak intensities of *m*/*z* 2792, 11687, 17271 and 28120 for 4 controls and 4 GVHD D0 representative samples. The darkness of the lines is proportional to the peak intensity.

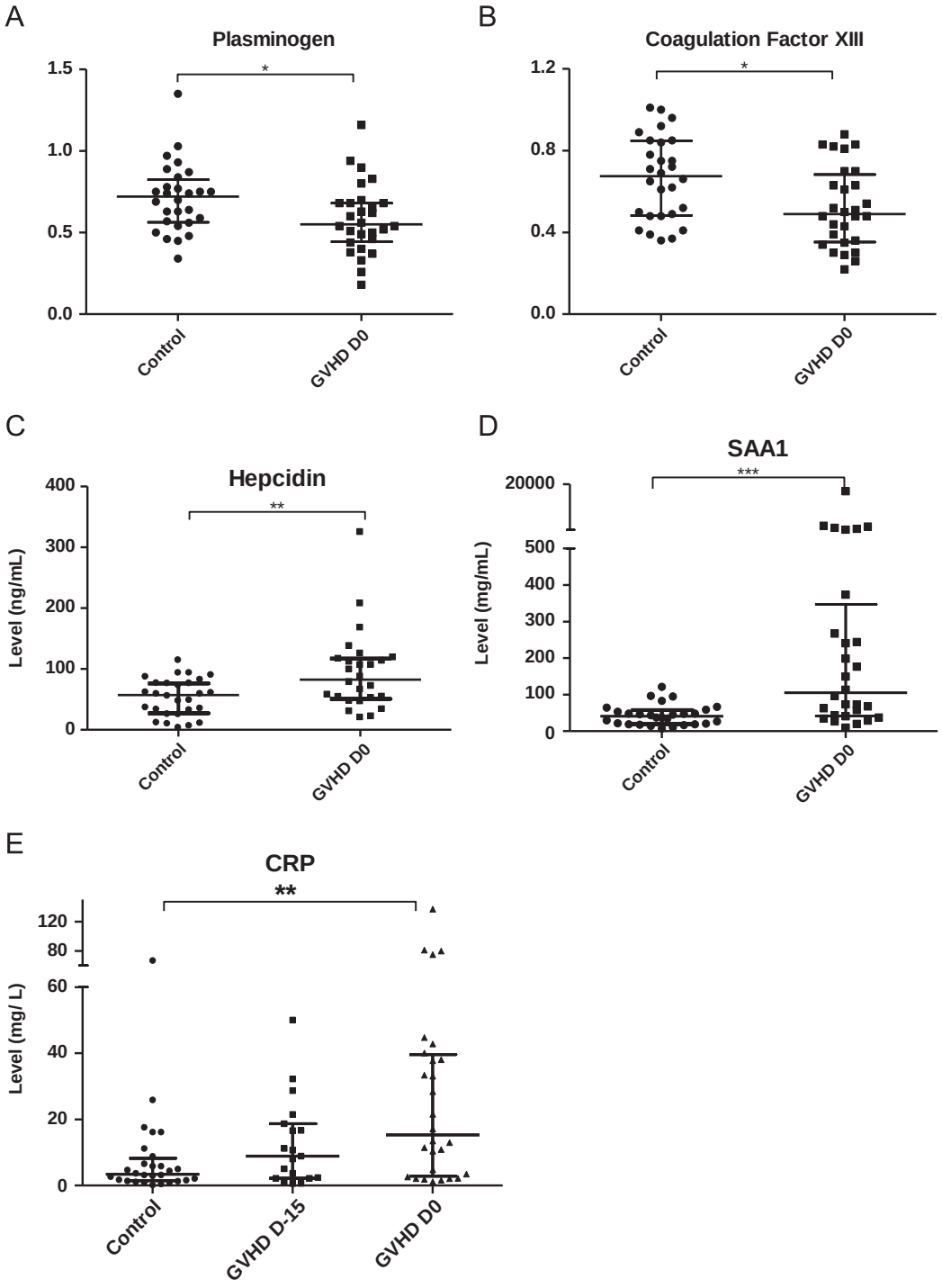

Fig. 3. Confirmation of biomarker candidates identified by the three proteomic approaches.> Protein levels of each potential biomarkers obtained by quantitative assays were compared between control and GVHD samples. *p*-Values were calculated using the Mann–Whitney test. * $p < 0.05$; ** $p < 0.01$; *** $p < 0.001$.
- Confirmation of statistically significant differences between groups for Plasminogen (A) and Coagulation factor XIII (B) as observed by 2D-DIGE. Protein abundance was determined by Western Blot after normalization of each band intensity value against two reference samples.
- Confirmation of statistically significant differences between groups for hepcidin (C) and SAA1 (D) as observed by SELDI-TOF-MS. LC-MS/MS and ELISA were applied to measure hepcidin and SAA levels, respectively.
-Confirmation of statistically significant difference between groups for CRP (E) as observed by 2D-LC-MS-MS. Protein levels were measured by immunoturbidimetric assay.

suggests that plasma proteins involved in multiple processes such as T-cell alloreactivity, inflammation, tissue damage and repair might be altered with the disease. Moreover, many papers reported thrombotic and hemostatic disorders after HSCT while inflammation linked to aGVHD could be associated with higher risk of thrombosis [43,44]. Inflammation and coagulation are processes mediated by the appearance of intercellular adhesion molecules on endothelia, and of various inflammatory mediators released [45–49]. Indeed, acute GVHD with gastrointestinal damage presents an increased risk of bleeding by tissue cells and leucocytes in response to tissue aggression. As widely described particularly in the case of myeloablative conditioning, aGVHD is initiated by tissue damages mainly caused by the underlying disease and the conditioning-related toxicity. Endothelial cell

Table 3
Correlation coefficients for proteins analysed by clinical assay, WB, ELISA and LC-MS/MS in aGVHD D0 samples.

	CRP[a]	SAA1[c]	HAMP[d]	FGB[a]	FGB[b]	PLG[b]	F13B[b]	F1+2[c]	HRG[b]	SAA4[b]
CRP[a]	/	/	/	/	/	/	/	/	/	/
SAA1[c]	**0.74*****	/	/	/	/	/	/	/	/	/
HAMP[d]	**0.62*****	NS	/	/	/	/	/	/	/	/
FGB[a]	**0.58****	**0.52****	**0.54****	/	/	/	/	/	/	/
FGB[b]	NS	NS	NS	**0.59*****	/	/	/	/	/	/
PLG[b]	**−0.41***	NS	NS	NS	NS	/	/	/	/	/
F13B[b]	**−0.44***	NS	NS	NS	**0.41***	**0.55****	/	/	/	/
F1+2[c]	NS	**−0.41***	NS	NS	NS	NS	NS	/	/	/
HRG[b]	NS	NS	NS	NS	NS	**0.49****	NS	NS	/	/
SAA4[b]	NS	NS	NS	NS	NS	NS	**0.45***	NS	NS	/
APOAI[c]	NS	NS	**−0.42***	NS	NS	NS	NS	NS	**0.40***	NS

NS: not significant.
F1+2: Prothrombin Fragment 1+2.

* $p < 0.05$.
** $p < 0.01$.
*** $p < 0.001$.
[a] Concentration determined by clinical assay.
[b] Normalised band volume from Western blot analysis.
[c] Concentration determined ELISA.
[d] Concentration measured by LC-MS/MS.

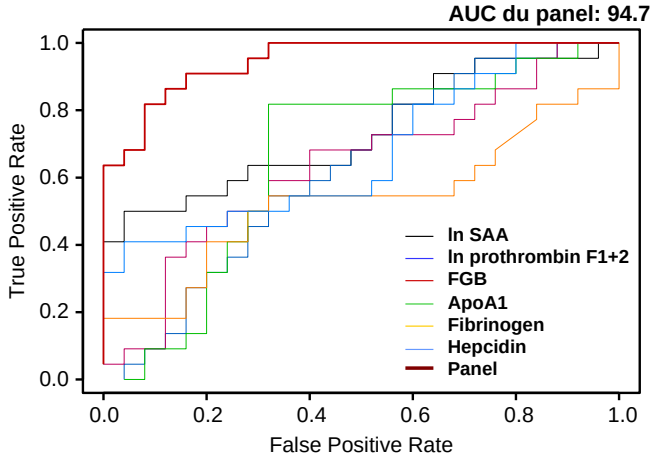

Fig. 4. Representation of ROC curves of the 6 individual biomarkers and the composite panel.

impairment leads to tissue factor and cytokine release, and subsequent antigen-presenting cell activation (e.g. macrophages and dendritic cells). Intestinal endothelium injuries are particularly important for the amplification of the immune process due to the direct contact with bacterial products such as lipopolysaccharides (LPS) that stimulate macrophages. Consequently, elevation of proinflammatory proteins levels such as IL-6 and TNF-α that are secreted by damaged tissues and activated immune cells, induces production of acute phase reactants [50]. Indeed, elevation of CRP levels has already been reported as predictive marker of HSCT complications and GVHD [51]. The serum amyloid A protein family members are involved in the regulation of inflammatory processes, lipid metabolism and lipid transport, and are mainly associated with plasma high density lipoproteins [52]. SAA1 is an acute phase reactant, thus it is not surprising to observe a positive correlation with CRP and fibrinogen levels (Table 3). As SAA1 release occurs within the first hour after acute injury [53,54], it is interesting to note that its level already increase 15 days before symptom appearance ($p=0.06$), unlike those of CRP and fibrinogen. Actually, Urieli-Shoval et al. reported an extrahepatic expression of SAA mRNA and protein in epithelial cells of many histologically normal human tissues, such as small and large intestine and skin epidermis [55]. Thus, early elevation of SAA before GVHD onset might result from early tissue leakage. Increase of IL-6 levels might also explain the elevation of plasma hepcidin concentration [56]. Wu et al., recently described that macrophages also produced hepcidin in response to LPS [57]. Furthermore, increase of hepcidin levels, an inhibitor of iron absorption, might also result from the disruption of iron homeostasis related to T-lymphocyte-inflicted tissue damage in the aGVHD process [58].

In addition, IL-6 and TNF-α are important mediators of inflammation-induced coagulation [59–61]. Indeed, they promote fibrin generation in severe inflammatory state, both systemically and locally. In aGVHD, the "cytokine storm" and APCs activation favour complex interaction between incompatible donor and recipient immune cells which results in donor T-cell activation/differentiation and IL-2 induced T-cell expansion. This leads to subsequent recruitment of cytotoxic effectors in different sites such as skin, gastrointestinal tract and liver tissue injuries, amplifying previous endothelium injuries. This results in a systemic and severe inflammatory response accompanied by excessive coagulation activation which leads to consumption of clotting factors and widespread depositions of fibrin. Indeed, we observed a decrease of antithrombin III and prothrombin levels in the LC-MS^E analysis and coagulation factor XIII level as well as increased levels of prothrombin fragments (F1+2), derived from prothrombin activation, that demonstrate an activation of the coagulation cascade. Pihusch et al. previously described that aGVHD with gastrointestinal damage presented an increased risk of bleeding that is associated with a decreased level of factor XIII, a protein stabilizing the fibrin clot [43]. This could be the result of a higher consumption of factor XIII at the site of damaged tissue. In parallel to this thrombotic process, plasminogen levels, a precursor of plasmin that is acting on the dissolution of fibrin blood clot, were found to decrease during aGVHD. It is probably due to its higher consumption in response to the excessive release of plasminogen activator by injured epithelium. This phenomenon leads to hyperfibrinolysis. Thus, aGVHD is a pathological process associated with both thrombotic and hyperfibrinolytic disorders. On the other hand, levels of HRG, a binding factor of plasminogen and fibrinogen as well as a negative acute phase reactant, also decrease with aGVHD onset due to acute state of inflammation [62]. HRG possesses a multifunctional role in different physiological processes, among others coagulation/fibrinolysis and modulation of cell adhesion to T-cells [62]. Thus, depletion of HRG could

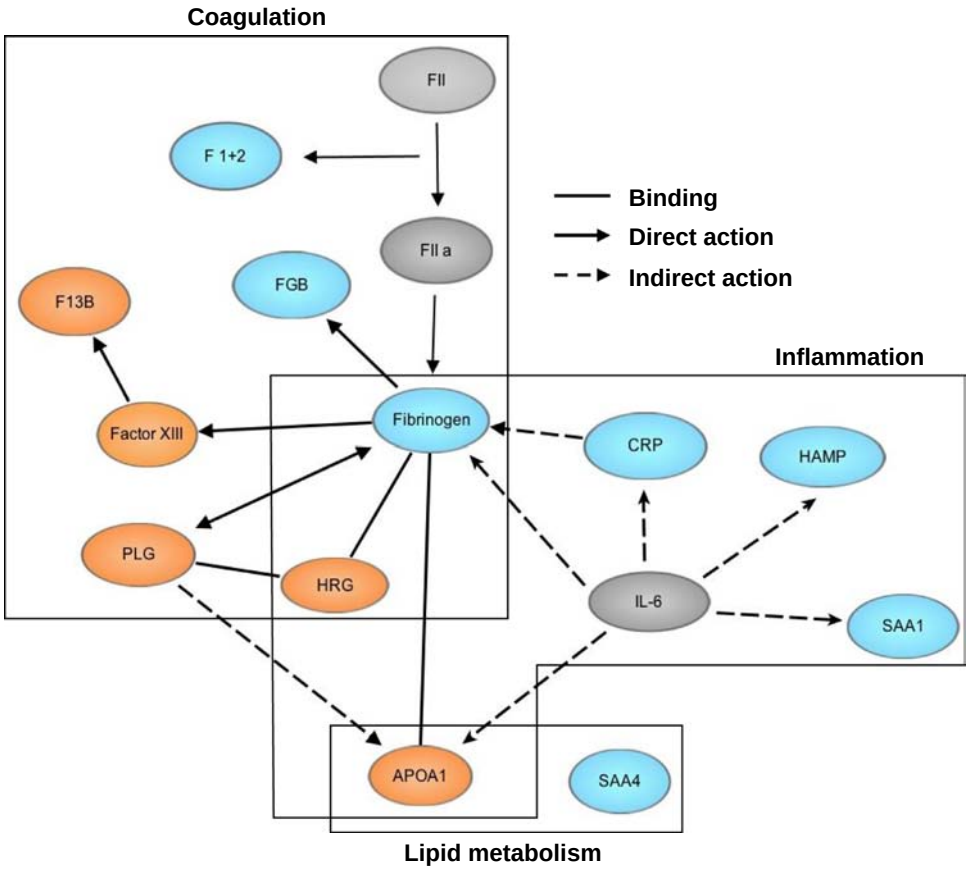

Fig. 5. Schematic representation of discovered biomarker interactions generated by Ingenuity Pathway Analysis software. Proteins are classified according to the main biological processes in which they are involved. Colors indicate level changes in aGVHD samples compared to control (blue upregulation; orange downregulation; grey protein level not determined in our study). FII: Prothrombin, FIIa: Thrombin, IL-6: Interleukin 6. (For interpretation of the references to color in this figure legend, the reader is referred to the web version of this article.)

contribute to the induction of coagulation and fibrinolysis cascades in GVHD [63].

In addition, fibrinogen, a dimeric 330 kDa plasma protein composed of two alpha, beta and gamma chains is a central protein of coagulation and inflammation (Fig. 5). Indeed, under the action of thrombin, fibrinopeptide A and B are cleaved from fibrinogen, releasing soluble fibrin monomers that form insoluble fibrin polymers stabilized by coagulation factor XIII [64]. In parallel, fibrinogen is an acute phase reactant that increases in inflammatory situations. Indeed, elevation of fibrinogen levels has already been associated with early HSCT complications [49]. However, the increase of fibrinogen level with aGVHD onset in this study was somewhat less significant than the increase of CRP. This suggests that inflammation-dependent stimulation of fibrinogen release is counterbalanced by its consumption through coagulation activation. Moreover, as a consequence of hyperfibrinolytic status, fibrinogen beta chain fragment levels as potential fibrin degradation products increase as observed by 2D-DIGE and LC-MS/MS^{E}.

Additionally, proteins levels of lipid metabolism were also altered with aGVHD occurrence. Indeed, apolipoprotein A1 is a protein involved in lipid metabolism by participating in the reverse transport of cholesterol from tissues to the liver. In addition, HDL associated with Apo A-I is a negative acute phase reactant which was found to decrease by at least 25% during acute inflammation [65] explaining its lower level at the time of aGVHD onset. Indeed, it plays an inhibitory role by interacting with activated T-cells and interfering with monocyte activation responsible for IL-1 and TNF-alpha release [66]. Changes of specific isoforms of Apo A-I levels between pre- and post-GVHD samples have already been observed by Wang et al. using intact protein analysis system [24].

SAA4, a protein of the serum amyloid A family, is constitutively expressed and is a constituent of normal, non acute phase high-density lipoprotein (HDL). The role of SAA4 is not well understood but it does not seem to be associated with acute phase inflammation as SAA1 and SAA2 are [67,68]. Indeed, no correlation was found between SAA4 and SAA1 and CRP levels. As reported previously [69], expression of SAA4 can be induced in human monocyte/macrophage cell lines [70] as well as in histologically normal human tissues such as small and large intestine or skin epidermis [55]. This might explain its increased levels with aGVHD occurrence as a consequence of cell damage.

Besides protein level changes observed at the time of aGVHD onset, it is worth noting that some biomarkers levels already varied before symptom development. Indeed, protein levels evaluated in samples taken 15 days before GVHD onset were found already modified compared to control samples, suggesting that early signs of aGVHD could be detected at the subclinical level. Thus, these proteins should be investigated as potential early diagnosis biomarkers of aGVHD.

Finally, we evaluated the capability of the candidate biomarkers to correctly discriminate patients with and without aGVHD. The composite biomarker panel generated by multivariate logistic regression provided a superior probability of correctly classify patients with and without aGVHD (AUC 0.95) compared to the best marker considered individually, SAA (AUC 0.74). This result

demonstrates that proteomic approaches are useful tools to identify a set of biomarkers, which can improve the disease diagnosis compared to the use of a single marker. As perspectives, the proposed biomarker panel should be investigated at early stage of GVHD, validated on a larger cohort of patients and challenged against GVHD related-diseases. We consider that the strength of the protein panel proposed is the very attractive AUC provided and the easiness to implement those protein assays in routine clinical biology laboratory.

Acknowledgments

MDB is Télévie Research Fellow, PL, MPM and FB are Senior Research Associate at the National Fund for Scientific Research (FNRS) Belgium. This work was financially supported by the National Fund for Scientific Research (FNRS), the "Télévie" and the "Fonds Leon Frederic". We thank the proteomic and bioinformatic platforms of the GIGA-Research Center.

Appendix A. Supporting information

Supplementary data associated with this article can be found in the online version at http://dx.doi.org/10.1016/j.talanta.2014.03.017.

References

[1] J.L. Ferrara, J.E. Levine, P. Reddy, E. Holler, Lancet 373 (2009) 1550–1561.
[2] B.R. Blazar, W.J. Murphy, M. Abedi, Nat. Rev. Immunol. 12 (2012) 443–458.
[3] G. Socie, B.R. Blazar, Blood 114 (2009) 4327–4336.
[4] V.T. Ho, R.J. Soiffer, Blood 98 (2001) 3192–3204.
[5] G. Socie, C. Schmoor, W.A. Bethge, et al., Blood 117 (2011) 6375–6382.
[6] C. Cutler, S. Li, V.T. Ho, et al., Blood 109 (2007) 3108–3114.
[7] F. Baron, M.B. Maris, B.M. Sandmaier, et al., J. Clin. Oncol. 23 (2005) 1993–2003.
[8] F. Baron, M. Labopin, D. Niederwieser et al., Leukemia (2012).
[9] P.J. Martin, J.D. Rizzo, J.R. Wingard et al., Biol. Blood Marrow Transplant. (2012).
[10] H.J. Deeg, Blood 109 (2007) 4119–4126.
[11] K.M. Sullivan, Graft-vs-host disease, in: K.G. Blume, S.J. Forman, F.R. Appelbaum (Eds.), Thomas' Haematopoietic Cell Transplantation, Blackwell Publishing Ltd, Oxford, United Kingdom, 2004, pp. 635–664.
[12] E. Willems, S. Humblet-Baron, O. Dengis, L. Seidel, Y. Beguin, F. Baron, Bone Marrow Transplant. (2010).
[13] K.W. Chik, K. Li, H. Pong, M.M. Shing, C.K. Li, P.M. Yuen, J. Pediatr. Hematol. Oncol. 25 (2003) 960–964.
[14] R.M. Dean, T. Fry, C. Mackall, et al., J. Clin. Oncol. 26 (2008) 5735–5741.
[15] S. Paczesny, O.I. Krijanovski, T.M. Braun, et al., Blood 113 (2009) 273–278.
[16] J.W. Chien, X.C. Zhang, W. Fan, et al., Blood 119 (2012) 5311–5319.
[17] S. Thiant, M. Labalette, J. Trauet, et al., Bone Marrow Transplant. 46 (2010) 1374–1381.
[18] E.M. Weissinger, E. Schiffer, B. Hertenstein, et al., Blood 109 (2007) 5511–5519.
[19] J.L. Ferrara, A.C. Harris, J.K. Greenson, et al., Blood 118 (2011) 6702–6708.
[20] M.M. Imanguli, J.C. Atkinson, K.E. Harvey, et al., Exp. Hematol. 35 (2007) 184–192.
[21] R. Srinivasan, J. Daniels, V. Fusaro, et al., Exp. Hematol. 34 (2006) 796–801.
[22] T. Kaiser, H. Kamal, A. Rank, et al., Blood 104 (2004) 340–349.
[23] S. Paczesny, T.M. Braun, J.E. Levine, et al., Sci. Transl. Med. 2 (2010) 13ra12.
[24] H. Wang, S.G. Clouthier, V. Galchev, et al., Mol. Cell. Proteomics 4 (2005) 618–625.
[25] T. Hori, Y. Naishiro, H. Sohma, et al., Blood 111 (2008) 4403–4412.
[26] E.M. Weissinger. Multicenter, Prospective and Blind Validation of Acute Graft-versus-Host-Disease-Specific Proteomic Patterns in a Large Patient Cohort: Prediction of Acute GvHD Grade III and IV. In: 38th Annual Meeting of the European Group for Blood and Marrow Transplantation. ((Eds.) (Geneva, Switzerland, 2012).
[27] A.C. Harris, J.L. Ferrara, T.M. Braun, et al., Blood 119 (2012) 2960–2963.
[28] J.E. Levine, B.R. Logan, J. Wu, et al., Blood 119 (2012) 3854–3860.
[29] R. Etzioni, N. Urban, S. Ramsey, et al., Nat. Rev. Cancer 3 (2003) 243–252.
[30] L. Guerrier, V. Thulasiraman, A. Castagna, et al., J. Chromatogr. B Analyt. Technol. Biomed. Life Sci. 833 (2006) 33–40.
[31] I.K. Fodor, D.O. Nelson, M. Alegria-Hartman, et al., Bioinformatics 21 (2005) 3733–3740.
[32] F. Quesada Calvo, M. Fillet, J. Renaut, et al., J. Proteome Res. 10 (2011) 4291–4301.
[33] F. Francis, F. Guillonneau, P. Leprince, et al., J. Insect Physiol. 56 (2010) 575–585.
[34] M. De Bock, D. de Seny, M.A. Meuwis, et al., Talanta 82 (2010) 245–254.
[35] V. Houbart, G. Cobraiville, F. Lecomte, B. Debrus, P. Hubert, M. Fillet, J. Chromatogr. A 1218 (2011) 9046–9054.
[36] G.H. Li, P.D. Arora, Y. Chen, C.A. McCulloch, P. Liu, Med. Res. Rev. 32 (2010) 999–1025.
[37] D. Nikitovic, P. Katonis, A. Tsatsakis, N.K. Karamanos, G.N. Tzanakakis, IUBMB Life 60 (2008) 818–823.
[38] C.T. Esmon, Br. J. Haematol. 131 (2005) 417–430.
[39] T. Yamada, T. Miida, Y. Itoh, T. Kawai, M.D. Benson, Clin. Chim. Acta 251 (1996) 105–112.
[40] T. Yamada, A. Wada, T. Yamaguchi, Y. Itoh, T. Kawai, J. Clin. Lab. Anal. 11 (1997) 363–368.
[41] J.H. Antin, J.L. Ferrara, Blood 80 (1992) 2964–2968.
[42] S. Paczesny, J.E. Levine, T.M. Braun, J.L. Ferrara, Biol. Blood Marrow Transplant. 15 (2009) 33–38.
[43] R. Pihusch, C. Salat, P. Gohring, et al., Br. J. Haematol. 117 (2002) 469–476.
[44] D. Davalos, K. Akassoglou, Semin Immunopathol. 34 (2012) 43–62.
[45] T. Matsumoto, H. Wada, H. Nishiyama, et al., Clin. Appl. Thromb. Hemost. 10 (2004) 341–350.
[46] M. Pihusch, Semin. Hematol. 41 (2004) 93–100.
[47] A.A. Petrolla, H.M. Lazarus, S.A.H. Unique, Thrombotic and hemostatic complications associated with allogeneic hematopoietic stem cell transplantation, in: H.M. Lazarus, M.J. Laughlin (Eds.), Allogeneic Stem Cell Transplantation, Humana Press, 2010, pp. 695–715.
[48] A. Pinomaki, L. Volin, L. Joutsi-Korhonen, et al., Bone Marrow Transplant. 45 (2010) 730–737.
[49] Y. Han, L. Zhu, A. Sun, et al., Ann. Hematol. 90 (2011) 1201–1208.
[50] H. Baumann, J. Gauldie, Immunol. Today 15 (1994) 74–80.
[51] S. Fuji, S.W. Kim, T. Fukuda, et al., Biol. Blood Marrow Transplant. 14 (2008) 510–517.
[52] C.M. Uhlar, A.S. Whitehead, Eur. J. Biochem. 265 (1999) 501–523.
[53] E. Malle, F.C. De Beer, Eur. J. Clin. Invest. 26 (1996) 427–435.
[54] K.P. McAdam, R.J. Elin, J.D. Sipe, S.M. Wolff, J. Clin. Invest. 61 (1978) 390–394.
[55] S. Urieli-Shoval, P. Cohen, S. Eisenberg, Y. Matzner, J. Histochem. Cytochem. 46 (1998) 1377–1384.
[56] E. Nemeth, E.V. Valore, M. Territo, G. Schiller, A. Lichtenstein, T. Ganz, Blood 101 (2003) 2461–2463.
[57] X. Wu, L.M. Yung, W.H. Cheng, et al., PLoS One 7 (2012) e44622.
[58] H.J. Deeg, E. Spaulding, H.M. Shulman, Leuk. Lymphoma 50 (2009) 1566–1572.
[59] T. van der Poll, H.R. Buller, H. ten Cate, et al., N. Engl. J. Med. 322 (1990) 1622–1627.
[60] T. van der Poll, M. Levi, C.E. Hack, et al., J. Exp. Med. 179 (1994) 1253–1259.
[61] J.M. Stouthard, M. Levi, C.E. Hack, et al., Thromb. Haemost. 76 (1996) 738–742.
[62] I.K. Poon, K.K. Patel, D.S. Davis, C.R. Parish, M.D. Hulett, Blood 117 (2010) 2093–2101.
[63] A.L. Jones, M.D. Hulett, C.R. Parish, Immunol. Cell Biol. 83 (2005) 106–118.
[64] M.W. Mosesson, J. Thromb. Haemost. 3 (2005) 1894–1904.
[65] D. Burger, J.M. Dayer, Autoimmun. Rev. 1 (2002) 111–117.
[66] N. Hyka, J.M. Dayer, C. Modoux, et al., Blood 97 (2001) 2381–2389.
[67] A.S. Whitehead, M.C. de Beer, D.M. Steel, et al., J. Biol. Chem. 267 (1992) 3862–3867.
[68] D.M. Steel, G.C. Sellar, C.M. Uhlar, S. Simon, F.C. DeBeer, A.S. Whitehead, Genomics 16 (1993) 447–454.
[69] N. Upragarin, W.J. Landman, W. Gaastra, E. Gruys, Histol. Histopathol. 20 (2005) 1295–1307.
[70] S. Urieli-Shoval, R.L. Meek, R.H. Hanson, N. Eriksen, E.P. Benditt, Am. J. Pathol. 145 (1994) 650–660.